Proceedings of DETC'02
2002 ASME Design Engineering Technical Conferences
September , 2002, Montreal, BC, Canada

DETC2002/DFM-XXXXX

TOWARD FAILURE MODELING IN COMPLEX DYNAMIC SYSTEMS: IMPACT OF DESIGN AND MANUFACTURING VARIATIONS

Irem Y. Tumer
Systems Health and Safety
Computational Sciences Division, MS 269-3
NASA Ames Research Center
Moffett Field, CA 94035-1000
Phone: 650-604-2976
Email: itumer@mail.arc.nasa.gov

Daniel A. McAdams
Department of Mechanical and Aerospace Engineering
and Engineering Mechanics
University of Missouri-Rolla
Rolla, Missouri 65409-0050
Phone: 573-341-4494
Email: dmcadams@umr.edu

ABSTRACT

When designing vehicle vibration monitoring systems for aerospace devices, it is common to use well-established models of vibration features to determine whether failures or defects exist. Most of the algorithms used for failure detection rely on these models to detect significant changes during a flight environment. In actual practice, however, most vehicle vibration monitoring systems are corrupted by high rates of false alarms and missed detections. Research conducted at the NASA Ames Research Center has determined that a major reason for the high rates of false alarms and missed detections is the numerous sources of statistical variations that are not taken into account in the modeling assumptions. In this paper, we address one such source of variations, namely, those caused during the design and manufacturing of rotating machinery components that make up aerospace systems. We present a novel way of modeling the vibration response by including design variations via probabilistic methods. The results demonstrate initial feasibility of the method, showing great promise in developing a general methodology for designing more accurate aerospace vehicle vibration monitoring systems.

Keywords

Vehicle health monitoring, variation modeling, Monte Carlo simulation, tolerance design, vibration analysis.

Designing Vehicle Health Monitoring Systems

In this work, the goal is to design effective vehicle health monitoring systems. The current focus is in assuring that correct models of system input signals are used for the algorithms and metrics used for failure detection. This paper explores one aspect of modeling input signals in such systems, namely, the consideration of statistical variations in the system response variable that is being monitored. In this light, the following subsections present some backgound research on vehicle health monitoring systems, presents examples of the types of variations encountered in such systems, and discusses the need to incorporate probabilistic models to account for such variations. Then, the use of probabilistic methods (e.g., Monte Carlo simulation) is explored with a simple example in design, and compared to more traditional variation analysis techniques. Next, a lumped parameter dynamic model is presented for a complex cam-follower system used in this paper, followed by an analysis of vibration data obtained from such a model. Finally, the Monte Carlo simulation technique is used to vary a subset of the design parameters. The effect on the vibration response is explored to determine whether probabilistic methods can be used to model the inherent variations observed in the dynamic response of complex systems.

Background and Objective

Failures in rotating machinery for high-risk aerospace applications are unacceptable when they result in catastrophic ac-

cidents, and undesirable when they result in high maintenance costs. In an attempt to detect any anomalous behavior during flight for increased safety, most aircraft manufacturers and operators are moving towards installing vehicle health monitoring systems. Despite the big push to make these systems standard onboard aircraft, false alarms and missed detections still remain a serious concern, making their reliability questionable and their operation costly in practice. One of the main reasons for the high rate of false alarms and missed failures is the lack of a statistically significant sample of baseline and failure signatures from which generalizations can be made. Specifically, since failure events are rare in such highly-maintained systems, there is no knowledge of the distribution of responses they could generate.

Recent work at NASA Ames Research Center has demonstrated that the statistical variations in baseline (healthy) data as well as faulty data must be accounted for to assure accurate anomaly detection in aircraft vibration-monitoring systems (Huff et al., 2000; Huff et al., 2002a; Tumer and Huff, 2000; Tumer and Huff, 2001; Huff et al., 2002b). In this work, we address the mismatch between modeled responses and empirical observations by developing statistically-accurate models that take variations into account. The specific objective is to explore probabilistic approaches to generate a reliable distribution of vibration responses using lumped-parameter dynamic models. If such an approach proves feasible, more accurate models of healthy and faulty aircraft vibration data will be developed and used as signal models for vibration monitoring systems.

Observed Variations in Vibration Signatures

For rotating machinery, vibration signals are excellent indicators of developing failures and defects in rotating components such as gears, bearings, shafts, rotors, etc. Each of the rotating components emanate specific frequencies that appear in the vibration signals; any changes in the amplitude and frequency content of these signatures, or the occurrence of sidebands or additional frequencies, is indicative of potential variations and defects. The types of variations of interest in this work include those that are inherent from the design and manufacturing processes (e.g., tolerances, assembly variations, surface roughness and waviness errors), material defects, cracks, and other point defects on the rotating components (Tumer and Huff, 2001; Huff et al., 2002a; Tumer and Huff, 2000). In this paper, we focus on variations introduced during design and manufacturing, effectively introducing a stochastic nature to the modeling parameters such as stiffness, mass, and damping.

Examples of such variations have been found throughout our research. As a first example, Figure 1 shows a schematic of a helicopter transmission for an OH58 helicopter (Lewicki and Coy, 1987), as well as a plot of experimental data we have collected using a test rig which houses such a transmission box (Huff et al., 2000). The different lines correspond to four different assembly instances where the data were collected. Within each instance, three variables were varied (namely torque, mast lift and mast bending forces). As shown, the overall vibration levels (total power) vary significantly depending on the test conditions defined by the four experimental variables (Huff et al., 2000). As a second example, Figure 2 shows a theoretical plot of the frequency spectrum from one of the gear systems contained in the helicopter transmission, based on our empirical observations (Huff et al., 2002b). The geometry of the gear system (epicyclic gears) includes four smaller gears (planet gears) revolving around a larger gear (sun gear) (Smith, 1999). The exact epicyclic gear mesh frequency appears at frequencies clustered around the theoretical frequency value due to the unequal spacing between planet gears. The spacing between the smaller gears is subject to design variations, which can result in different frequency distributions, which in turn can invalidate the signal modeling assumptions (Huff et al., 2002b).

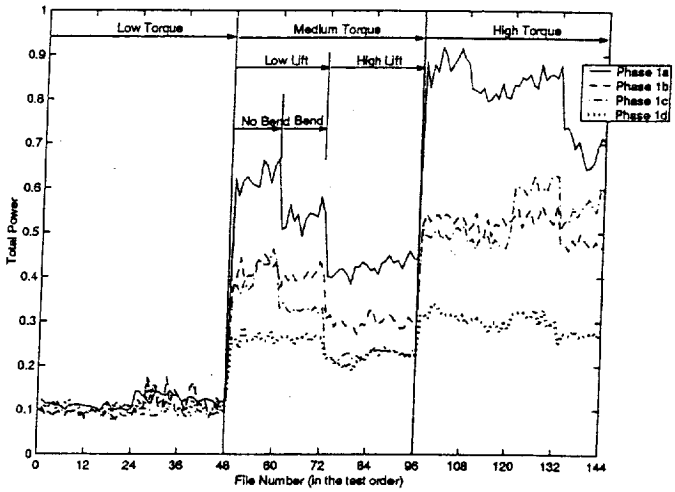

Figure 1. Baseline Variations in Overall Vibration Levels in a Rotorcraft Transmission.

Probabilistic Variation Analysis in Design

A significant degree of variation is introduced during the design, manufacturing, and assembly of components that make up aircraft systems. Standard tolerance variation analysis methods used in design address this variability by predicting the total variation in the final system (Creveling, 1997). Because we are starting from similar variation sources, this approach will be explored and extended here to dynamic models of complex systems to predict the variation in vibration response characteristics.

A simple mechanical assembly is shown in Figure 3, where

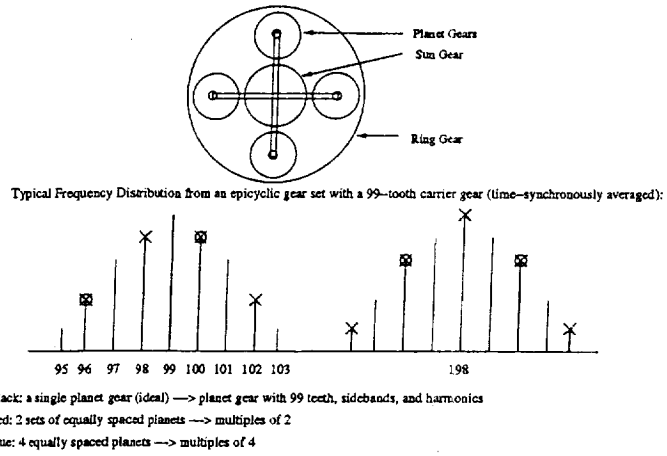

Figure 2. Typical Variation in the Frequency Spectrum due to Design Variations in Epicyclic Gears.

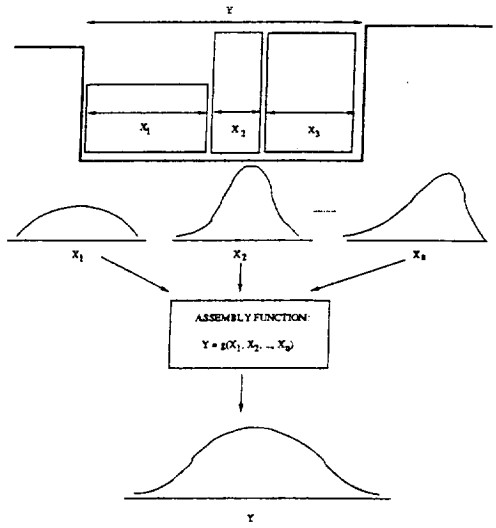

Figure 3. Application of Statistical Methods to Determine Critical Assembly Tolerances.

three rectangular blocks of dimension X_1, X_2, and X_3 are designed and manufactured to fit within the allowable space of dimension Y. Due to the inherently probabilistic nature of the manufacturing process, each of the dimensions is assigned specific tolerances based on a distribution set by the designer (either based on empirical manufacturing data or process capability specifications (Creveling, 1997).) Typically, statistical tolerance analysis techniques are applied to geometric models of such assemblies to predict the magnitude and range of the variations in critical assembly features.

Figure 3 also shows the application of a probabilistic model (e.g., Monte Carlo (MC) simulation) to perform tolerance analysis for each manufacturing and design parameter (Hammersley and Handscomb, 1964; Creveling, 1997). Values of each parameter X_i are drawn from a random distribution, and then combined through some assembly function (a model) to determine the corresponding values for the final variable of interest. The statistical moments are then computed for the resultant values, which in turn are used to determine the probability distribution that matches the final assembly variable Y. The following section illustrates the application of Monte Carlo methods to variation modeling using a simple design example.

Monte Carlo Methods: Review and Example

Conceptually, Monte Carlo simulation is simple and elegant (Metropolis and Ulam, 1949; Hammersley and Handscomb, 1964). Consider some function

$$y = f(x_1, x_2, ..., x_n) \tag{1}$$

where, y is a known function of random variables $x_1, x_2, ..., x_n$. Each x_i has a known random nature, assuming that all the x_i's are statistically independent. The question we wish to answer (or simulate) is: what is the random nature of y?

To determine the random nature of y, a random sample is generated for each x_i. Using the known function f, y is generated. Depending on the information needed from the random nature of y (perhaps a mean μ and standard deviation σ, or the number of times y exceeds some value out of 1000 trials, etc.) the value of y or some sort of frequency count is recorded.

As an example, consider the design of a helical coil spring to achieve some specific spring constant k. The relation between the performance k and the design variables is

$$k = \frac{d^4 G}{8D^3 N} \tag{2}$$

with d the wire diameter out of which the spring is made, G the shear modulus of the spring material, D the diameter of the spring (helix diameter) and N the total number turns or coils of the spring. As a first pass, a deterministic model with $d = 1.5$ mm, $G = 79$ GPa, $D = 18.0$ mm, and $N = 13$ turns gives $k = 660N/m$.

Of course, the values of d, G, D, and N do not always take on the same precise values for each spring that is manufactured. Thus, a more accurate (with regard to how well it represents reality) model would be one which considers the way the variations of d, G, D, and N cause a variation in k.

For cases where the function f is simply represented and smooth enough to provide second derivatives, a low order approximation for the mean of y can be expressed as below, with the partial derivatives evaluated at $x_i = \mu_i$ (Hahn and Shapiro, 1994; McAdams and Wood, 2000):

$$\mu_y = f(\mu_{x_1}, \mu_{x_2}, \cdots, \mu_{x_n}) + \frac{1}{2}\sum_{i=1}^{n} \frac{\partial^2 f}{\partial x_i^2} Var(x_i). \quad (3)$$

Similarly, a low order approximation for the variance of y can be expressed as:

$$Var(y) = \sum_{i=1}^{n} \left(\frac{\partial f}{\partial x_i}\right)^2 Var(x_i). \quad (4)$$

Equations (3) and (4) can be applied to Equation (2) to yield:

$$\mu_k = \frac{\mu_d{}^4 \mu_G}{8\mu_D{}^3 \mu_N} + \frac{1}{2}\frac{12\mu_d{}^2 \mu_G}{8\mu_D{}^3 \mu_N} Var(d) + \frac{1}{2} 0 Var(G) + \frac{1}{2}\frac{12\mu_d{}^4 \mu_G}{8\mu_D{}^5 \mu_N} Var(D) + \frac{1}{2}\frac{2\mu_d{}^4 \mu_G}{8\mu_D{}^3 \mu_N{}^3} Var(N). \quad (5)$$

Similarly, for the variance,

$$Var(k) = \left(\frac{4\mu_d{}^3 \mu_G}{8\mu_D{}^3 \mu_N}\right)^2 Var(d) + \left(\frac{\mu_d{}^4}{8\mu_D{}^3 \mu_N}\right)^2 Var(G) + \left(\frac{-3\mu_d{}^4 \mu_G}{8\mu_D{}^4 \mu_N}\right)^2 Var(D) + \left(\frac{-\mu_d{}^4 \mu_G}{8\mu_D{}^3 \mu_N{}^2}\right)^2 Var(N). \quad (6)$$

Substituting $d = 1.5\ mm$, $G = 79\ GPa$, and $D = 18.0\ mm$ for the average values μ_d, μ_G, μ_D, μ_N and taking $Var(d) = 2.5 \times 10^{-5}\ mm$, $Var(G) = 6.9\ GPa$, $Var(D) = 18.6 \times 10^{-3}\ mm$, and $Var(N) = 1.87 \times 10^{-3}$ turns (Shigley and Mischke, 2001) for the variations gives $\mu_k = 660\ N/m$ and $Var(k) = 27{,}600\ N/m$. Translating this into a mechanical tolerance using a common convention (tolerances $= 3\sigma_x = 3\sqrt{(Var(x))}$) gives $498\ N/m$.

Using Eqs. (3) and (4) allows designers a starting point to understand, and compensate for, the effects of variation. Nevertheless, this approximate approach has a number of key shortcomings that become apparent and critical as we explore more complex systems and the compound effects of different types of variation. Of critical importance here are that 1) as engineering models become complex and computational, Eqs. (3) and (4) fail to provide tractable analysis, and 2) these two equations give us limited, if at times misleading, information about the probability distribution function of y.

Consider the relation $y = sin(x)$. Using Eqs. (3), (4), and taking x to be a random variable from a standard normal distribution gives $\mu_y = 0$ and $\sigma_y = 1$. Such a result may lead a designer to the notion that y can be modeled as a variable from standard normal distribution. If this notion was used to make parameter specifications or expectations of failure, important errors could occur. Shown in Fig. 4 is a plot of the probability density function of y. A key restriction of this theorem is that the mapping of y=f(x) be one to one; a restriction violated by our simple spring example (Eisen, 1969).

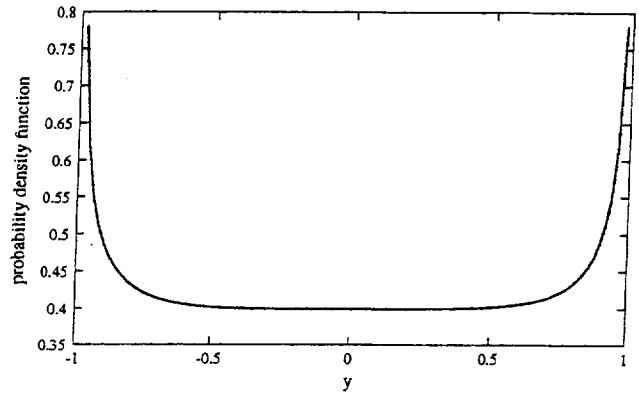

Figure 4. The probability density function of y where $y = cos(x)$ and x is a standard normal variable.

Returning to our spring example, we now use Monte Carlo simulation to explore the variation in k as a function of the variations in d, G, D, and N. The histogram in Fig. 5 is generated performing a Monte Carlo simulation as outlined in the second paragraph of this section. Based on this simulation, there were no springs (out of a sample run of 100,000 springs) that fell below $k = 660 - 498\ N/m$ and above $k = 660 + 498\ N/m$ (taking the tolerance $498\ N/m$). This is compared to 270 (.27% *from three − sigma tolerancing*) as implied by the analytic approximation. The standard deviation of the Monte Carlo simulated springs is $17.5\ N/m$ leading to a 3σ tolerance of $52.5\ N/m$. The significant difference between the Monte Carlo simulated variation and that approximated by Eq. 4 is due to the non-linearity of Eq. 2. Also, this comparison highlights the potential for engineering errors (in this case likely of a conservative nature) that would be made based on simple, linearized, analytic models such as those given by Eqs. 3 and 4.

This short review and comparison of approaches to representing variation in design highlights some of the advantages of Monte Carlo simulation. In summary, with the minimal penalty of some computation time, Monte Carlo simulation provides more useful information for the designer. Based on this insight, we use Monte Carlo simulation to explore how different sources of variation combine in more complex systems to affect the overall response and performance of a system.

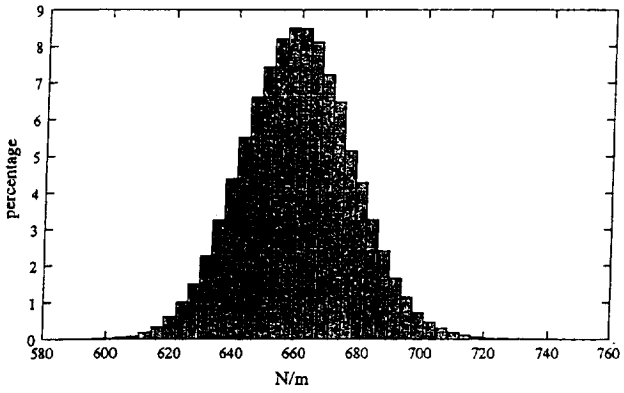

Figure 5. Histogram of k values generated using Monte Carlo simulation.

Application: Cam-Follower Vibration Model

A lumped-parameter, seven degree-of-freedom (fourteenth-order) model of a cam follower is used in this paper as an example of a complex nonlinear system. The cam-follower system is shown in Figure 6, and a schematic of the model is shown in Figure 7, adapted from (Grewal and Newcombe, 1988). The parameter values for the cam-follower system were taken from (Grewal and Newcombe, 1988), and are listed in Table 1. The equations of motion for the model are:

$$I_c\ddot{\theta} = -C_{sf}(\dot{\theta}_c - \dot{\theta}_i) - K_{sf}(\theta_c - \theta_i) - C_b\dot{\theta}_c - T_c, \quad (7)$$

$$M_c\ddot{y}_1 = -C_{vs}\dot{y}_1 - K_{vs}y_1 - F_c\cos\Phi + F_p, \quad (8)$$

$$M_r\ddot{y}_2 = -C_f(\dot{y}_2 - \dot{y}_3) - K_f(y_2 - y_3) + F_c\cos\Phi - F_p, \quad (9)$$

$$M_f\ddot{y}_3 = C_f(\dot{y}_2 - \dot{y}_3) + K_f(y_2 - y_3) - C_4(\dot{y}_3 - \dot{y}_4) - K_4(y_3 - y_4) - F_w - F_{cb}, \quad (10)$$

$$M_3\ddot{y}_4 = C_4(\dot{y}_3 - \dot{y}_4) + K_4(y_3 - y_4) - C_3(\dot{y}_4 - \dot{y}_5) - K_3(y_4 - y_5), \quad (11)$$

$$M_2\ddot{y}_5 = C_3(\dot{y}_4 - \dot{y}_5) + K_3(y_4 - y_5) - C_2(\dot{y}_5 - \dot{y}_6) - K_2(y_5 - y_6) \quad (12)$$

and,

$$M_1\ddot{y}_6 = C_2(\dot{y}_5 - \dot{y}_6) + K_2(y_5 - y_6) - C_1\dot{y}_6 - K_1y_6, \quad (13)$$

where θ_i is the input position, K_{sf} and C_{sf} model the damping and stiffness of the cam drive shaft, C_b accounts for friction losses in the drive shaft bearing, M_c is the mass of the cam itself, and, I_c is the cam moment of inertia about its center of rotation. To account for the flexure of the shaft, a shaft stiffness, K_{vs}, and a damping, C_{vs} have been added. The offset of the cam follower from the center of the rotation of the cam is e, K_h accounts for deformation at the roller-cam interface and M_r is the mass of the roller. The inertia of the roller is assumed to have a negligible effect on the rotational dynamics of the system. The mass of the follower is M_f, with K_f and C_f the structural stiffness and damping of the follower, respectively. C_{cb} accounts for the friction at the interface of the follower and the follower guide, F_{cb} is the force that results for this friction, and, F_w is the external load on the follower. The spring has been modeled as three elements to approximate the distributed mass of the spring. K_1, K_2, and K_3 are the distributed spring constants. The structural damping of the spring is approximated as C_1, C_2 and C_3. M_1, M_2, and M_3 are the mass of the spring. The state-space equations were integrated using a Runge-Kutta integration routine. A simple harmonic motion (SHM) cam profile with a maximum rise of $.0254m$ is used. The cam is assumed to rotate at a deterministic 1500 *RPM* (25 *Hz*). The numerical values for the constants used in the simulation of cam operation are presented in Table 1.

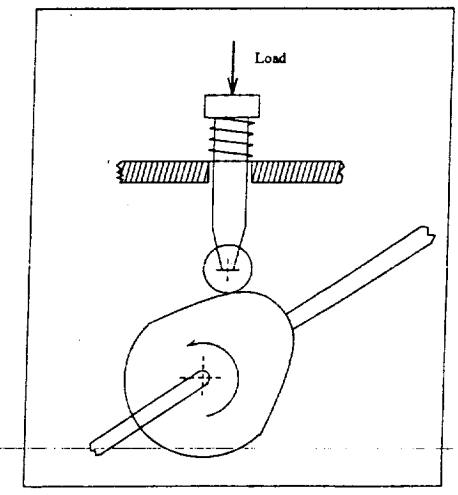

Figure 6. Schematic of cam-follower modeled

In Figure 8, the velocity and acceleration responses of the cam follower (from variable y_3 in Figure 7) are shown. The dashed line shows the idealized follower velocities and accelerations as determined by differentiating the cam profile. The solid line adds the realism of system mass, stiffness, and the resulting dynamics. In contrast, Figure 9 shows the velocity and acceleration responses of the cam follower with a profile error of 25 μm and a surface roughness of 2.0 μm added to the cam profile. The profile error is modeled using a deterministic offset. The pro-

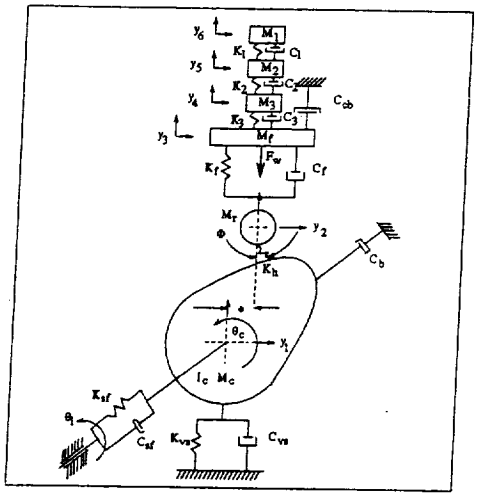

Figure 7. The lumped parameter dynamic model of the cam-follower system.

Table 1. Constant Values for the Cam-Follower Dynamic Model.

Element	Variable	Value
cam moment of inertia	I_c	$.00091034 kg/m^2$
cam shaft rotational damping	C_{sf}	$.01356 N \cdot m \cdot s/rad$
cam shaft rotational stiffness	K_{sf}	$22600 N \cdot m/rad$
drive shaft friction	C_b	$.113 N \cdot m \cdot s/rad$
cam mass	M_c	$.5017 Kg$
cam shaft horizontal damping	C_{vs}	$752.9 N \cdot s/m$
cam shaft horizontal stiffness	K_{vs}	$2.6e^9 N/m$
system preload	F_p	$266.62 N$
follower stiffness	K_f	$175.1e^6 N/m$
follower mass	M_f	$.340 kg$
follower damping ratio	η_f	$.75$
follower damping	C_f	$\eta_f 2\sqrt{M_f K_f}$
external follower load	F_w	$100 N$
return spring stiffness	$K_{1,2,3}$	$63000 N/m$
return spring mass	$M_{1,2,3}$	$.0227 kg$
return spring damping ratio	η_{rs}	$.075$
return spring damping	$C_{1,2,3}$	$\eta_{rs} 2\sqrt{M_1 K_1}$
cam eccentricity	e	$.01905 m$

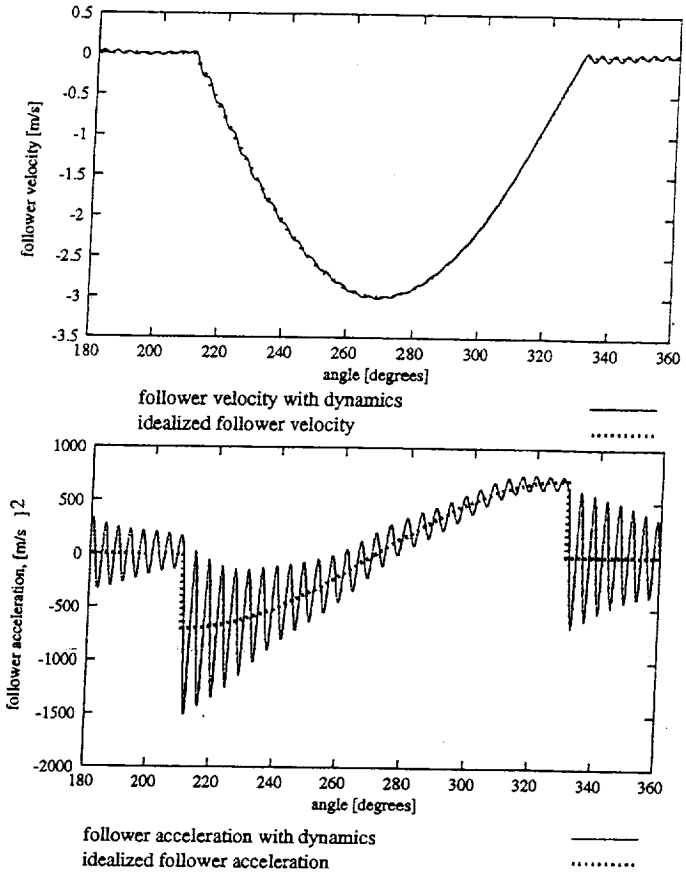

Figure 8. Follower velocity and acceleration as a function of cam rotation with ideal surface smoothness and no profile tolerance on the cam.

file error was simulated on the cam surface by the addition of a sinusoid of $t_p/3 sin(n\theta)$. In this case, t_p is the profile tolerance and n was taken to be small compared to the forcing frequency ($1500 RPM$) and large with respect to the step size of the simulation code. The surface roughness is modeled using a random number generator and transformation techniques to simulate the surface roughness.

The addition of these geometric variations cause minimal change in follower velocity as a function of cam angle. However, the simulations show that a geometric variation in the cam causes a significantly different acceleration, with a large magnitude, in the follower. The effective higher frequency and magnitude follower will cause significantly different vibrations on the system. Of particular relevance to our effort to simulate failure modes is that an increase in follower acceleration is related to an increase in the wear rate of the cam and follower (Rothbart, 1956).

Probabilistic Cam-Follower Vibration Model

Exploring the vibrational impact of variations in parameters such as spring stiffness provides a different simulation challenge. Parameter values of components vary from cam system to cam system. For example, the spring constant on several cam systems would be distributed similarly to the distribution in Figure 5. But, in a single cam system, these variations are static in time. The core research question is whether these non-time varying parameter variations combine to give time-varying vibration signals that are falsely indicative of system failure. In many important cases, this question is simply answered. Above, the static (with respect to a single cam) variation of the cam profile from the ideal cause a change in the vibrational behavior of the system. In general, however, this question remains unanswered.

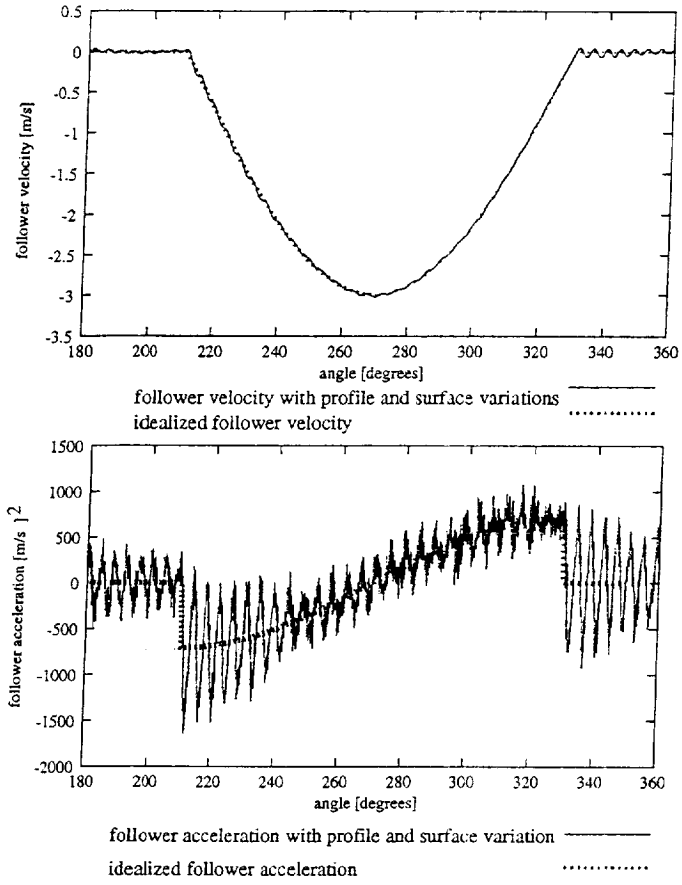

Figure 9. Follower velocity and acceleration as a function of cam rotation with profile and surface variation on the cam.

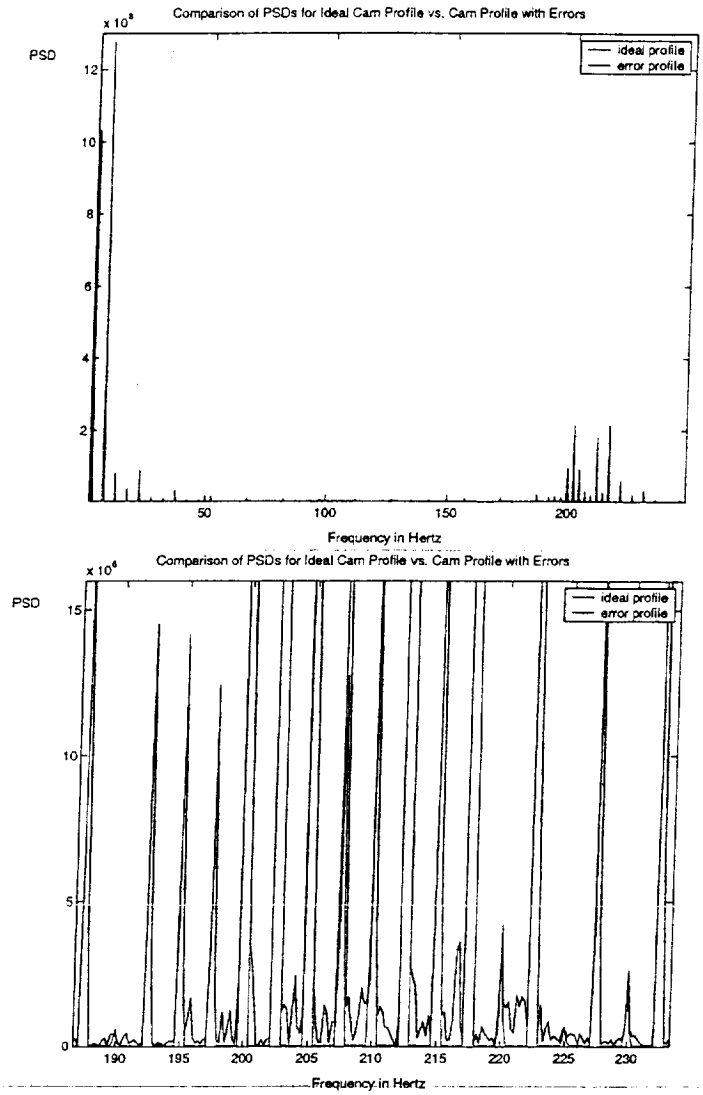

Figure 10. Comparison of Power Spectral Densities for an Ideal Cam Profile vs. a Cam with profile tolerance and surface roughness added (high-frequency range zoomed-in).

Analysis of Cam-Follower Vibration Signatures

Prior to analyzing the effect of design variations on the vibrational response, the vibration signature needs to be understood to decide on a possible set of features (vibration metrics) that will be used to monitor system performance and indicate the occurrence of failures. A small sample of the simulated cam-follower vibration responses is shown in Figures 8 and 9 for half a revolution (for an ideal cam and a cam with profile errors, respectively). 12 revolutions of these signals are used to analyze the frequency content, with a sampling frequency of $10000Hz$ (Nyquist frequency cut-off is $5000Hz$.)

The frequency content of these signals is shown in Figure 10. The first plot shows the entire set of frequencies computed from the two signals. Based on a careful analysis, the only difference in the frequency content due to the addition of profile and surface errors manifests itself in the higher frequency range. The second plot shows a zoomed-in portion of the higher-frequency range where the difference due to the two signals can be seen clearly. In general, the addition of the profile and surface errors introduces frequencies in the noise range, as well as increasing the overall power levels.

Many possibilities exist for selecting a feature set for the purposes of monitoring changes in the vibration signatures (Smith, 1999; Lewicki and Coy, 1987; Tumer and Huff, 2001). In this paper, we first focus on the most obvious and the most standard vibration monitoring feature, namely, the global measure of vibration levels. This measure can be computed as the area under the power spectral density plot in the frequency do-

main (equivalent to the variance in the time domain by Parseval's theorem.) Because most of the changes due to the addition of surface errors to the cam profile are observed in the higher-frequency range shown in Figure 10 ($\approx 177Hz$ to $250Hz$), we select the total power in this range the vibratin metric of interest for this study. Many other metrics are available and will be explored in the future.

Anlaysis of the Impact of Design Variations

Next, the signals defined and analyzed in the previous subsection are varied using the Monte Carlo simulation method. In this case, both the signal from the ideal cam and from the cam with profile and surface errors are used to determine whether a random variation in the spring constant K (see model in Figure 7), similar to the helical spring explored in a previous section, will result in significant variations in the vibration metric of interest (e.g., total power in the high-frequency range).

The spring constant tolerance model is developed by analogy with the earlier example in the paper. The spring constant mean is taken as 21,000 N/m with a standard deviation of 2.65% (660/17.5 = 0.0265) or 567 N/m. Recall that the spring that we explored before had a mean of 660 N/m and a standard deviation of 17.5 N/m. The spring was chosen as the element to vary because we can develop a reasonable tolerance model for this element (unlike the damping), and it is likely to have larger affect on our vibrational response then one of other parameters.

$N = 200$ number of trials are generated using the Monte Carlo simulation method (minimum number of trials required (Creveling, 1997)). A plot of the selected vibration metric is shown in Figure 11 for the case of the ideal cam profile and the cam profile with errors. As observed, the overall vibration levels and the variance in these levels are significantly higher for the case of cam profile with errors.

The statistics (mean, standard deviation, skewness, kurtosis) of the vibration data generated using MC simulation are summarized in Table 2 for all of the frequency ranges for comparison. Using the high-frequency range once again, the ideal profile case results in a mean value of 62,967.00 and a standard deviation of 83.98, resulting in a tolerance of 251.95. The error profile case results in a mean value of 69,250.00 and a standard deviation of 3,468.50, resulting in a tolerance of 10,404.00 for the overall vibration metric. Recall from the earlier review of Monte Carlo techniques that the standard approach to computing tolerances (using Equations 3 and 4) based on the complex mathematical relationship between the design parameters (d, G, D, and N) and the vibration response (sum of the total power in $\ddot{y}_3$) would have been intractable and highly simplistic (linearized.) This computational approach provides the vehicle monitoring system designer with the possible ranges of acceptable values of the vibration monitoring metric, based on the random variation in the selected subset of design parameters. Figure 12 shows the statistical distribution of the high-frequency vibration power values for both cases (total number bins is 20.) As observed, the vibration metrics for both cases follow a normal distribution. However, the spread in the vibration metric computed from the case of cam profile with errors is much larger in value than the ideal cam profile case.

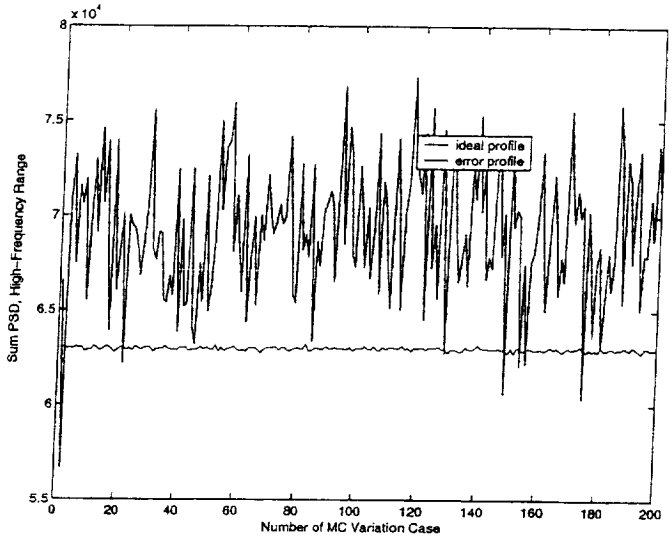

Figure 11. Total Power in the High-Frequency range for an Ideal Cam vs. a Cam with profile tolerance and surface roughness added.

Discussion

Several observations can be made based on these analysis results. First, in addition to the mean levels of the vibration metric being larger, the variance in the value of the vibration metric due to the variation of the spring constant is significantly larger in the case of the cam with surface errors. This implies a greater impact of design variations on the vibration response of the (more realistic) cam with profile and surface errors. As a result, the models used for vehicle health monitoring systems not only have to take the variation in the design parameters into account, but also model the profile and surface errors more accurately, which is nonexistent from current models.

Second, the effect of the random variation in the spring constant (K) variable on the vibration metric is quite significant, as observed by the high variance value. The mathematical relationship describing the vibration metric selected in this study would have to be modified to add the expected variation which has propagated through the complex dynamic system, and resulted in the computed variation. In addition, the values of the metric within the computed variation range will have to be stored to assure the

Table 2. Statistics of Total Power Changes due to MC simulation.

	Ideal Profile				Error Profile			
Freq Range	Mean	St Dev	Skew	Kurt	Mean	St Dev	Skew	Kurt
Total	231670.00	82.51	-0.23	3.35	249930.00	3468.4	-0.25	3.15
Low-Freq	163880.00	0.54	-0.06	3.07	164120.00	143.27	-0.21	3.03
High-Freq	62967.00	83.98	-0.22	3.35	69250.00	3468.5	-0.25	3.18

elimination of false alarms: in other words, training of the data must include the variation that has propagated through the system, so that anomalies are not identified incorrectly.

Let us revisit the situation described in Figure 1, where the four experimental factors (mast lift, mast bend, torque, and assembly) resulted in significant differences in vibration levels. The question those empirical observations brought up was whether any of these vibration levels were "acceptable". A probilistic approach as described in this paper will enable the designer to set the limits of the vibration levels according to the mathematical model of the OH58 test rig vibrations, which will then identify which of the test conditions fall within the acceptable limits of variation. A similar approach can be followed for the situation described in Figure 2, where the vibration metric would be the power level at each of the frequencies, and angular variations in the placement of the planet gears can be propagated through the system to determine further effects.

Conclusions and Future Work

This paper addresses the problem of incorrect modeling assumptions made when designing vehicle health monitoring systems, resulting in high rates of false alarms and missed detections. The specific problem that was addressed is the necessity of including the effect of statistical variations introduced during design and manufacturing of rotating machinery components that make up most aerospace systems. The propagation of such significant variations through the system and their effect on the final monitoring metric of interest is typically unknown, invalidating certain signal modeling assumptions. In this paper, probabilistic methods (e.g., Monte Carlo simulation) are used to describe the nature of the variations in the system response due to variations in a subset of design parameters. The results show significant variation that must be taken into account using probabilistic models.

The paper presents an initial feasibility of enhancing deterministic dynamic models of complex systems by combining them with probabilistic models. Only a subset of design parameters (those describing the spring constant K) were considered in this paper. For a more thorough analysis, we need to run a full MC simulation on all the parameters and then do a sensitivity analysis. Finally, the example uses a cam-follower system. Future work will attack the problem of high-risk aerospace systems with much more complex system models. Ongoing work focuses on developing finite difference models of such complex systems, which will be used to determine whether and how the design and manufacturing variations propagate through the system, and how they can be represented in the signal modeling assumptions for vehicle health monitoring systems.

REFERENCES

Creveling, C. 1997. *Tolerance design: a handbook for developing optimal specifications*. Prentice Hall PTR, New York, NY.

Eisen, M. 1969. *Introduction to Mathematical Probability Theory*. Prentice-Hall, Englewood Cliffs, New Jersey.

Grewal, P. S. and Newcombe, W. R. 1988. Dynamic performance of high-speed semi-rigid follower cam systems - effects of cam profile errors. *Mechanism and Machine Theory*, 23:121–133.

Hahn, G. J. and Shapiro, S. S. 1994. *Statistical Models in Engineering*. John Wiley and Sons, Inc., New York.

Hammersley, J. and Handscomb, D. 1964. *Monte Carlo Methods*. Wiley, New York, NY.

Huff, E., Tumer, I., Barszcz, E., Dzwonczyk, M., and McNames, J. 2002a. Analysis of maneuvering effects on transmission vibrations in an ah-1 cobra helicopter. *Journal of the American Helicopter Society*.

Huff, E., Tumer, I., Barszcz, E., Lewicki, D., and Decker, H. 2000. Experimental analysis of mast lifting and mast bending forces on vibration patterns before and after pinion reinstallation in an OH-58 transmission test rig. In *American Helicopter Society 56th Annual Forum*, Virginia Beach, VA.

Huff, E., Tumer, I., and Mosher, M. 2002b. Comparison of transmission vibration responses from oh-58c and ah-1 helicopters. *Journal of the American Helicopter Society*, In preparation.

Lewicki, D. and Coy, J. 1987. Vibration characteristics of OH58a helicopter main rotor transmission. *NASA Technical Paper*, NASA TP-2705/AVSCOM TR 86-C-42.

McAdams, D. A. and Wood, K. L. 2000. Tuning parameter tolerance design: Foundations, methods, and measures. *Research in Engineering Design*, 12(1):152–162.

Metropolis, N. and Ulam, S. 1949. The monte carlo method. *Journal of American Statistics*, 44(247):335–341.

Rothbart, H. A. 1956. *Cams: Design, Dynamics and Accuracy*. John Wiley & Sons, New York, New York.

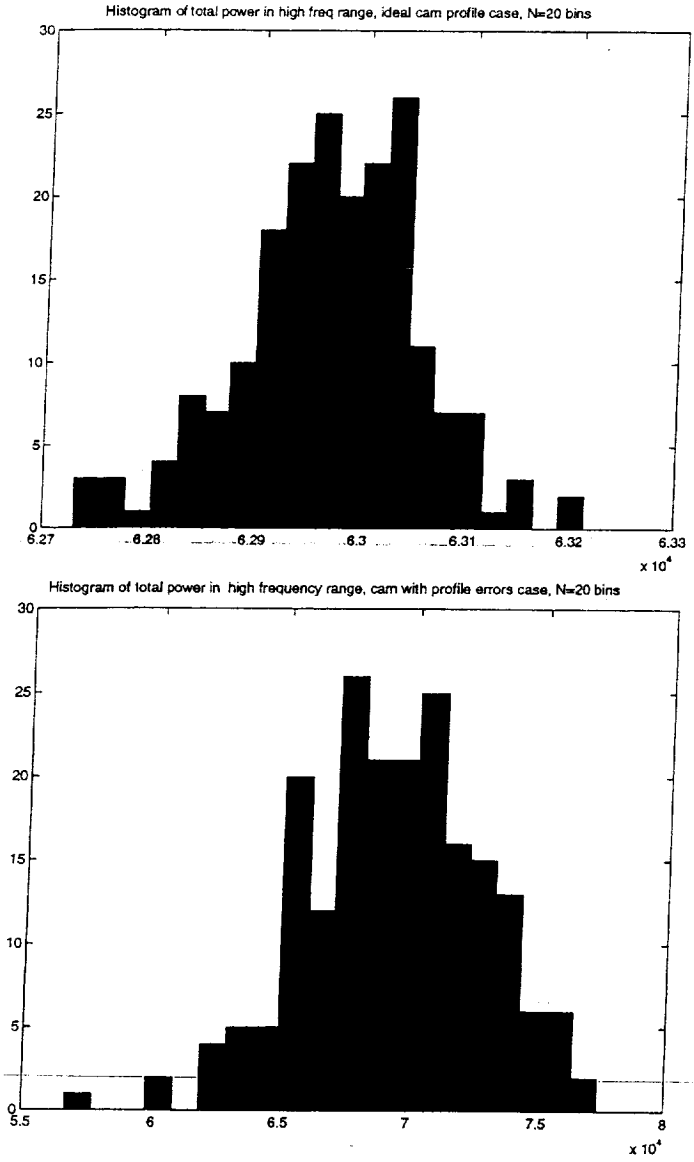

Figure 12. Histogram of the Probability Distribution of the Total Power in the High-Frequency range for an Ideal Cam vs. a Cam with profile tolerance and surface roughness added.

Shigley, J. E. and Mischke, C. R. 2001. *Mechanical Engineering Design*. McGraw Hill, St. Louis, MO, 6th edition.

Smith, J. 1999. *Gear Noise and Vibration*. Marcel Dekker.

Tumer, I. and Huff, E. 2000. Evaluating manufacturing and assembly errors in rotating machinery to enhance component performance. In *ASME Design for Manufacturing Conference*, volume DETC2000-DFM14006, Baltimore, MD.

Tumer, I. and Huff, E. 2001. Using triaxial vibration data for monitoring of helicoper gearboxes. In *ASME Mechanical Vibration and Noise Conference*, Pittsburgh, PA.